Chapter 7

Human *in vivo* longevity is reflected *in vitro* by differential metabolism as measured by ^{1}H-NMR profiling of cell culture supernatants

Pim Dekker, Axel Meissner, Roeland W. Dirks, P.E. Slagboom, Diana van Heemst, André M. Deelder, Hans J. Tanke, Rudi G.J. Westendorp, Andrea B. Maier

Mol Biosyst.. 2012 Jan [Epub ahead of print]

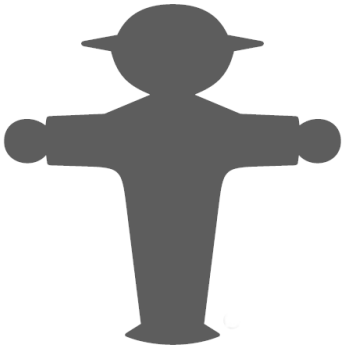

Summary

The offspring of nonagenarian siblings suffer less from age related conditions and have a lower risk of mortality compared with their partners. Fibroblast strains derived from such offspring in middle age show different *in vitro* responses to stress, more stress-induced apoptosis and less senescence when compared with strains of their partners. Aiming to find differences in cellular metabolism *in vitro* between these fibroblast strains, cell culture supernatants collected at 24-hours and five days were analyzed using ^{1}H nuclear magnetic resonance (NMR)-based metabolic footprinting. Between 24-hours and five days of incubation, supernatants of all fibroblast strains showed decreased levels of glucose, pyruvate, alanine-glutamine (ala-gln), valine, leucine, isoleucine, serine and lysine and increased levels of glutamine, alanine, lactate and pyroglutamic acid. Strains from offspring and their partners were compared using a partial least squares-discriminant analysis (PLS-DA) model based on the data of the five-day time point. The ala-gln and glucose consumption was higher for fibroblast strains derived from offspring when compared with strains of their partners. Also, production of glutamine, alanine, lactate and pyroglutamic acid was found to be higher for fibroblast strains derived from offspring. In conclusion, differences in NMR-based metabolic profiles of human cells *in vitro* reflect the propensity for human longevity of the subjects from whom these were derived.

Introduction

Life expectancy has dramatically increased in Western society, but there is much inter-individual variation in life expectancy (1). Healthy longevity has been shown to be a combination of genetic, environmental and chance factors. To study the phenotype and genetic component of healthy aging we designed the Leiden Longevity Study (LLS), in which families with exceptional longevity were recruited (2). Nonagenarian siblings and their offspring showed a lower risk of mortality than controls from their birth cohort. As compared with their partners, this offspring show a lower prevalence of myocardial infarction, hypertension and diabetes mellitus (3) and features such as preservation of insulin sensitivity with age and a beneficial glucose handling (4;5) and lipid metabolism (6). The contrast between offspring of nonagenarian siblings that express the propensity for longevity and their partners was also found to be reflected by cellular characteristics *in vitro*. In dermal fibroblast strains from offspring, oxidative stress induced less reactive oxygen species (ROS), less senescence, more apoptosis and slower growth speed when compared with strains from the partners of the offspring (7;8). Furthermore, cytotoxic T cell responses were more pronounced in offspring (9).

In accordance with other features of healthy metabolism we found that offspring had a lower thyroidal sensitivity to thyrotropin, affecting levels of the thyroid hormone, which is primarily responsible for regulation of protein, fat and carbohydrate metabolism (10). For model organisms it has been shown that caloric restriction extends life span, which has been suggested to be caused by a shift from carbohydrate to fatty acid metabolism. This is thought to result in decreased cellular damage, since fatty acid metabolism preferentially uses mitochondrial complex II, which is known to produce less damaging ROS than the other mitochondrial complexes I, III, IV and V (11). However, for humans not much is known about the relation between cellular metabolism and longevity.

We have already reported that skin fibroblast strains derived from offspring of nonagenarian siblings show a cellular phenotype *in vitro* that differs from their partners (7;8). We now aimed to investigate if these fibroblast strains also show differences in cellular metabolism *in*

vitro. To measure metabolic changes, we chose to measure the metabolites in the cell culture supernatants of the strains. Measurement of intracellular metabolites requires rapid quenching of metabolism and a time-consuming and often inadequate extraction and separation procedure (12). ^{1}H-NMR-based metabolic footprinting (13) of cell culture supernatants requires minimal sample preparation, thus introducing fewer artefacts (14). This methodology will therefore also allow better correlation with *in vivo* techniques. Here we describe the results of ^{1}H-NMR-based metabolic footprinting (13) of cell culture supernatants of human fibroblast strains *in vitro* from offspring and their partners.

Material and methods

Study design

The LLS was set up to investigate the contribution of genetic factors to healthy longevity by establishing a cohort enriched for familial longevity (2). From July 2002 to May 2006, 421 families were recruited consisting of 944 long-lived Caucasian siblings together with their 1671 of their offspring and 744 of the partners thereof. There were no selection criteria on health or demographic characteristics. Compared with their partners, the offspring were shown to have a 30% lower mortality rate and a lower prevalence of cardio-metabolic diseases (2;3). During the period November 2006 and May 2008, a biobank was established from fibroblasts cultivated from skin biopsies from 150 offspring-partner couples. Because it was expected that the difference in biological age between the offspring and partner groups would be relatively small, a relatively large sample size of 68 fibroblast strains from 34 couples was randomly chosen. In accordance with the Declaration of Helsinki we obtained informed consent from all participants prior to their entering the study. Good clinical practice guidelines were maintained. The study protocol was approved by the ethical committee of the Leiden University Medical Center before the start of the study.

Fibroblast Cultures

Four-mm skin biopsies were taken from the sun unexposed medial side of the upper arm. Fibroblasts were grown in D-MEM:F-12 (1:1) medium supplemented with 10% fetal calf serum (FCS, Bodinco, Alkmaar, the Netherlands, batch no. 162229), 1 mM MEM sodium pyruvate, 10 mM HEPES, 2 mM glutamax I, and antibiotics (100 Units/mL penicillin, 100 µg/mL streptomycin, and 0.25–2.5 µg/mL amphotericin B), all obtained from Gibco, Breda, the Netherlands. This medium will be referred to as standard medium. Fibroblasts were incubated at 37^{o}C with 5% CO_2 and 100% humidity. All cultures that are used in the present study were grown under predefined, highly standardized conditions and frozen at low passage as published earlier (7;15) Trypsin (Sigma, St Louis, MO, USA) was used to split fibroblasts using a 1:4 ratio each time they reached 80-100% confluence.

Experimental set-up

Experiments were set up in batches of maximally 10 fibroblast strains, which were thawed from frozen stocks on day zero. On day one, the medium was changed and on day four fibroblasts were passaged 1:4 and passaged further in equal numbers on days six and eight to have similar confluences for experiments. On day 11, 9x104 fibroblasts were seeded in 25 cm^2 tissue culture flasks for experiments and after overnight incubation with standard medium, fibroblasts were washed with serum-free medium and 3 ml serum-free medium per flask was added. Cell culture supernatants were collected at 24 hours and five days and stored at -70^{o}C. Cell-free/serum-free medium incubated at 37^{o}C with 5% CO_2 and 100% humidity for 24 hours and five days was used as control medium.

Plating efficiency

Plating efficiency could confound concentrations of metabolites in the cell culture supernatants. To test if plating efficiency between strains from offspring and partners was different, fibroblasts strains were also seeded in 96-well plates and fixed after four hours. Fibroblasts were washed with water and stained with 0.6 mg/ml Coomassie in 1:6 methanol/water overnight, washed again with water and air dried. Plates were then scanned with a high resolution Agfa XY-15 flatbed scanner (Agfa Gevaert, Mortsel, Belgium) and cells were counted automatically with the freely available image analysis software package

ImageJ 1.37v. No differences in plating efficiency were found (75±4% [mean±SD] and 76±4% for strains from offspring and partners, respectively, p=0.79).

NMR methodology

Preparation of cell culture supernatants for ^{1}H-NMR Spectroscopy

After thawing, cell culture supernatants were centrifuged with 3000g for 10 min at 4ºC for the removal of any cellular components. 540 µL supernatant was mixed with 60 µL of 1.5 M phosphate buffer (pH 7.4) in D2O containing 4.0 mM sodium 3-trimethylsilyl-tetradeuteriopropionate (TSP) and 2.0 mM NaN_3 (16). All reagents were purchased from Sigma-Aldrich, St Louis, MO, USA. The resulting samples were then centrifuged with 3000g for 10 min at 4ºC prior to manual transfer into 5 mm SampleJet sample tubes in 96 tube racks. Tubes were closed with polyoxymethylene (POM) balls and tube racks were placed on the sample changer where they were kept at 6ºC while queued for data acquisition.

NMR Data Acquisition and Processing

^{1}H-NMR data was obtained using a Bruker 600 MHz AVANCE II spectrometer equipped with a 5 mm TCI cryo probe and a z-gradient system; a Bruker SampleJet sample changer system was used for sample transfer. One-dimensional (1D) ^{1}H-NMR spectra were recorded at 300 K using the first increment of a NOESY pulse sequence (17) with presaturation (γB1 = 50 Hz) during a relaxation delay of 4 sec and a mixing time of 10 msec for efficient water suppression (18). Duration of 90 degree pulses were automatically calibrated for each individual sample using a homonuclear-gated nutation experiment (19) on the locked and shimmed samples after automatic tuning and matching of the probe head. 64 scans of 65,536 points covering 12,335 Hz were recorded and zero filled to 65,536 complex points prior to Fourier transformation, an exponential window function was applied with a line-broadening factor of 1.0 Hz. The spectra were manually phase and baseline corrected and automatically referenced to the internal standard (TSP = 0.0 ppm). Phase offset artefacts of the residual water resonance were manually corrected using a polynomial of degree 5 least square fit filtering of the free induction decay (FID) (20).

Multivariate Data Analysis of NMR Spectroscopic Data

A bucket table with a bucket size of 0.04 ppm was generated for the regions 10.0–5.1 and 4.5–0.2 ppm, respectively, using AMIX version 3.5 (Bruker Biospin, Germany). Buckets were normalized to a total area of 1.0 and metadata was included after import of the data into MS Excel (version 2003; Microsoft). For multivariate statistical analysis SIMCA-P+ (version 12.0, Umetrics, Sweden) software package was used. Since high abundant metabolites are generally the major source of the overall variability within the data, NMR variables were Pareto scaled and centred prior to PCA and PLS-DA analysis in order to emphasize variability of minor components. Variables were centred but not scaled for PLS-DA analysis after OSC filtering since the filtering step does remove variability not related to the classes investigated and hence already accentuate relevant minor components. Likewise, data for outlier detection was not scaled since outliers were defined as data with “abnormal” variability of specific variables on an absolute scale. For initial analysis and outlier detection PCA was performed using eight components. Outliers were identified based on scores (Hotelling’s T2 range) and distance of the observation in the training set to the X model plane values, as well as visual inspection of the individual NMR spectra during data processing. Spectra of insufficient quality due to poor water suppression or bad automated shim performance (broad lines) were excluded from the analysis. For OSC-filtering and PLS-DA analysis samples were categorized based on offspring/partner and time point, respectively. PLS-DA models were validated by random permutation of the response variable and comparison of the goodness of fit (R2Y and Q2Y) of 200 such models with the original model in a validation plot. R2Y and Q2Y of the original PLS models as well as intersects of the R2Y and Q2Y regression lines of the validation plots with the vertical axis were calculated as quality parameters. Relative changes in metabolites were identified based on coefficient plots and variable importance in the projection (VIP). The cutoff for changes to be considered significant was based on VIP and the confidence interval derived from jack knifing of the corresponding coefficients. Mean spectra were calculated from the original NMR data for individual classes of the obtained models in order to assist annotation of loadings and coefficient plots and to determine relative differences in metabolite concentrations between the classes and to determine relative differences in metabolite concentrations between the classes.

Results

Table 1 shows the characteristics of the randomly selected subset of subjects from whom fibroblast strains were tested. Partners and offspring were of similar age, height and weight.

Initial PCA model and metabolic footprinting of fibroblast strains dependent on incubation period

Principal component analysis (PCA) was applied to detect biochemical outliers and to identify variability within the data that correlates with offspring/partner status, time point and gender classification. After removal of spectroscopic outliers (Supplemental table 1), a PCA model

Table 1. Clinical characteristics of offspring and partners from the Leiden Longevity Study, representing a difference in biological age.

	Offspring n=34	Partners n=34
Demographic data		
Female	19	15
Age, years (mean±SD)	61.7 (6.7)	60.5 (7.5)
Anthropometric data		
Height, cm (mean±SD)	170 (8)	174 (9)
Weight, kg (mean±SD)	74 (13)	79 (14)
Current smoking – no./total known	3/27	8/29
Diseases		
Myocardial infarction – no./total known	0/33	0/33
Stroke – no./total known	1/33	0/33
Hypertension – no./total known	5/33	7/33
Diabetes mellitus – no./total known	1/32	2/32
Malignancies – no./total known	0/31	1/31
Chronic obstructive pulmonary disease – no./total known	1/32	1/33
Rheumatoid arthritis – no./total known	0/33	0/33

based on data from 134 of 144 samples (34 offspring strains, 34 partner strains, four cell-free controls, all taken at 24 hours and five days), was built using eight components with an explained variability of 97.9% and a predicted variation of 94.0%. Already in the scores plot of the first two principal components (PCs) two dominating clusters correlating with the incubation time of 24 hours and five days, respectively, can be identified as shown in Figure 1. A strong time-dependent discrimination was already found in the first components of the PCA model since depletion of the medium components and accumulation of waste products over time are expected as main source of variability due to cellular metabolism. Furthermore, cell-free/serum-free medium (from here on referred to as control medium) did not change over time and the corresponding data for these control samples were found in the scores plot as separate sub-cluster at one side of the 24-hour cluster. Hence, a time trajectory emerged as indicated in Figure 1, starting from the control medium on the left and progressing to the right within the scores plot showing the cell culture supernatants incubated for 24 hours and five days.

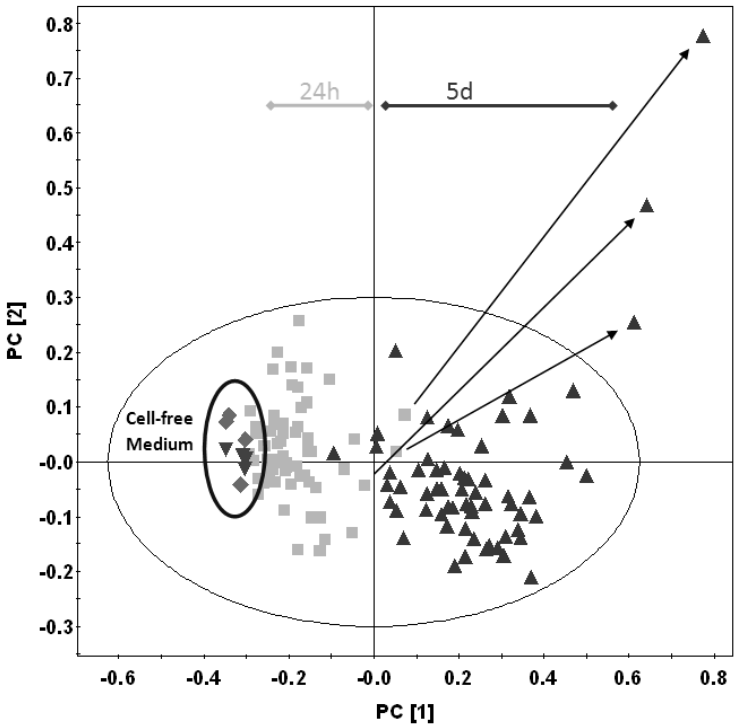

Figure 1. Scores plot of first two principal components from PCA model built from complete data set. Data points are labeled according to fibroblast culture incubation duration of 24 hours (■) and five days (▲) as well as cell-free medium incubated for 24 hours (◆) and five days (▼). Arrows indicate culture samples with accelerated metabolism (for details see text).

For detection of biological outliers, a separate PCA model based on centred but not scaled data was built using eight components. The scores (Hotellings T2 range) and distance of the observation in the training set to the X model plane values identified one outlier for the 24 hour incubation time point and three outliers for the five-day incubation time point (Supplemental figure 1). The three samples from the five-day time point, namely one male offspring, one female offspring and one female partner, respectively, already deviated from the other samples in the scores plot in Figure 1. The scores plot in Supplemental Figure 2 and closer investigation of the medium profiles for these three subjects showed deviations already for the 24h time point samples. The observed differences indicate accelerated metabolism for the fibroblasts of these three strains accompanied by increased lactate production. All identified biological outliers were excluded from further analysis.

The main metabolites responsible for the observed clustering in the initial PCA are shown in the loadings plot in Figure 2. In order to investigate the time dependent changes further, a separate PLS-DA two-class model was built with the time point as response variable. The scores plot of the first two components showed a clear discrimination between the two time points (Supplemental figure 3).

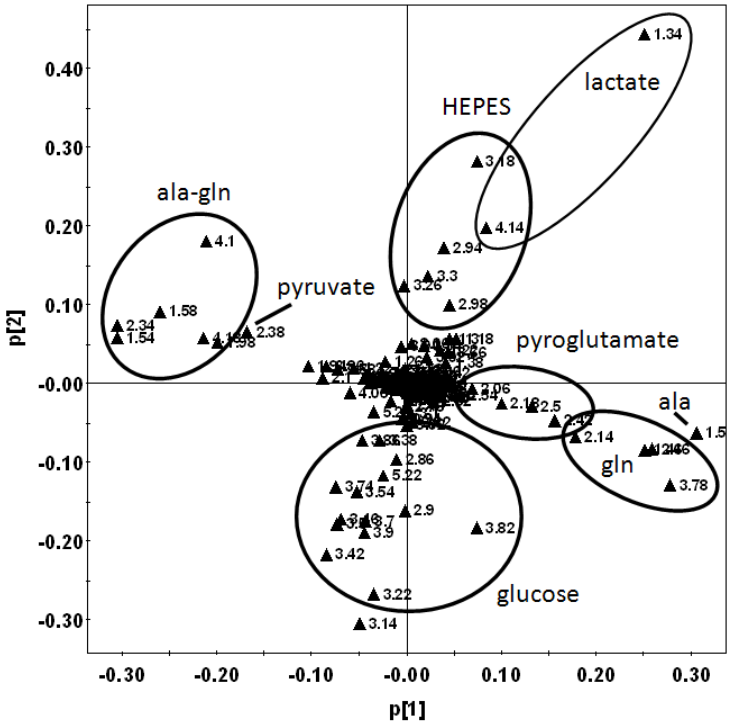

Figure 2. Loadings plot of first two principal components from PCA model built from complete data set. Main metabolites responsible for variability are annotated. Metabolites with negative p[1] loadings (left) are decreased in the five-day samples compared with the 24-hour samples, whereas metabolites with positive p[1] loadings (right) are increased in the cell culture supernatants of five days compared with those of 24 hours.

A cumulative R^2Y of 0.96 and Q^2Y of 0.94 were calculated for the model and the model validation plot showed intercepts of the R^2Y and Q^2Y regression lines with the vertical axis at 0.142 and -0.396, respectively, indicating a valid model. Based on coefficients (Supplemental figure 4) and loadings from this model the responsible metabolites for the discrimination of the two groups were identified. Decreased components in the five-day medium in comparison to 24-hour medium were grouped into energy metabolism compounds like glucose, pyruvate and the dipeptide ala-gln and amino acid building blocks like valine, leucine, isoleucine, serine and lysine. Increased metabolites in medium were lactate, alanine, glutamine, pyroglutamic acid, formic acid, glycine, 2-oxo-4-methyl pentanoic acid, 2-oxo-3-methyl pentanoic acid, 2-oxo-3-methyl butanoic acid and acetic acid. A direct link between ala-gln decrease and glutamine and pyroglutamic acid increase was established, suggesting ala-gln as an alternative energy source (Figure 3). An apparent increase of HEPES buffer was observed at the five-day time point when compared with the 24-hour time point. However, this increase can most likely be attributed to an inverse normalization effect, since consumption of major components will result in an apparent increase of invariant constituents after total area normalization. This is a well-known effect commonly observed in metabonomic analysis of normalized spectroscopic data (21;22).

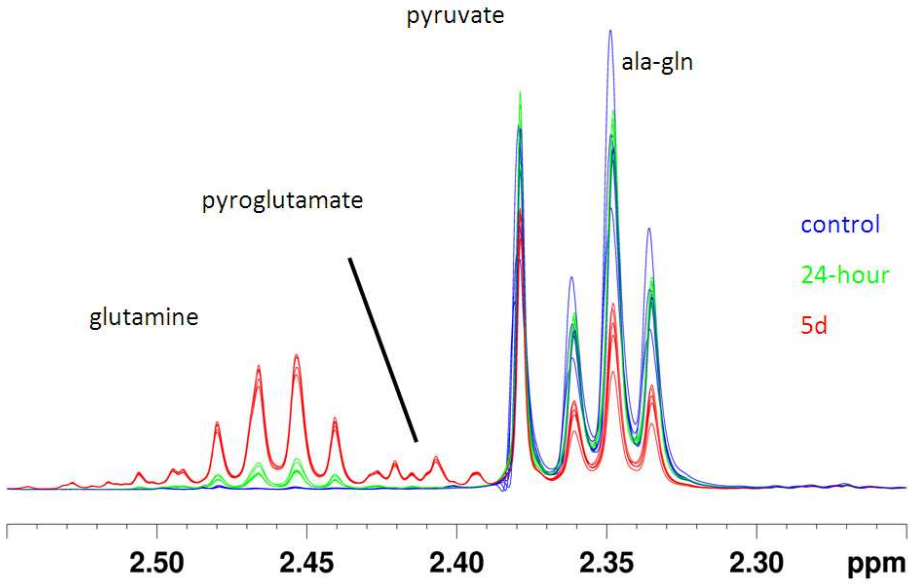

Figure 3. Excerpt of 1D NOESY spectra from representative traces (six each) of cell-free control medium (blue) and cell culture supernatant after 24 hours (green) and five days (red) incubation time, demonstrating link between ala-gln consumption and glutamine release.

PLS-DA model to detect differences in offspring/partner

Within the initial PCA model no additional clustering according to gender, age or offspring/partner classification was observed. To identify significant subtle differences between the metabolic profile of fibroblasts from offspring and partners, a PLS-DA model was built using data from the five-day time point. This time point was chosen to allow rather small differences to accumulate over time. However, the initial PLS-DA model did not discriminate between offspring and partner (data not shown). Therefore, a second PLS-DA two-class model after OSC-filtering using two components with a remaining sum of squares of 21.3% and an Eigenvalue of 11.1 was built. For two components, a cumulative R^2Y of 0.51 and Q^2Y of 0.32 were obtained and model validation showed intercepts of the R^2Y and Q^2Y regression lines with the vertical axis of the validation plot at 0.049 and -0.131, respectively, indicating a valid model. The OSC filtering step was independently validated using a leave-one-out cross validation procedure (see supplement material). Figure 4 shows the scores plot of the first and second components of this PLS-DA two-class model, indicating separation between offspring and partners with some degree of overlap between the two clusters. Based on coefficients and loadings from this model, molecular discriminators between metabolic footprint profiles of the fibroblast supernatants of offspring and partners were identified, as summarized in Table 2. The main differences were observed for metabolites involved in the energy metabolism.

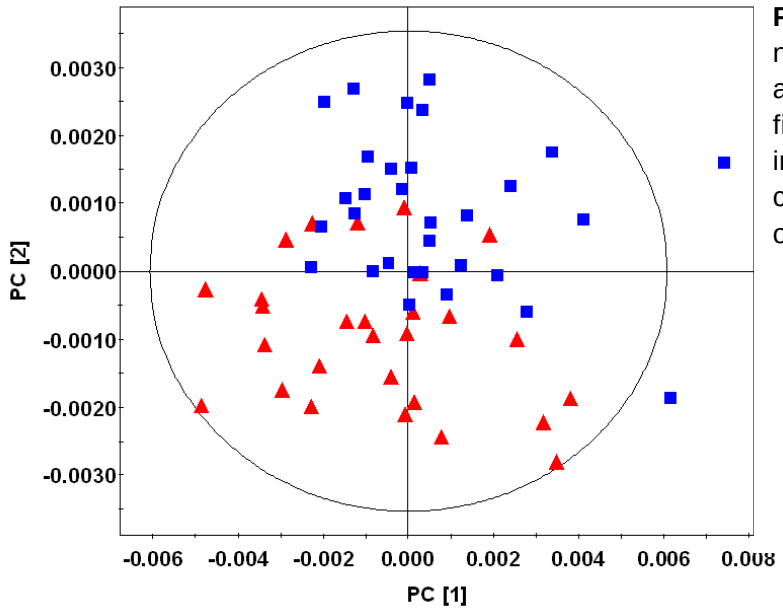

Figure 4. Scores plot of first two components from PLS-DA two-class model built after OSC filtering of NMR data from fibroblast cell culture supernatants after incubation for five days. Data points are coloured according to partner (■) and offspring (▲) classification, respectively.

Table 2. Metabolites in cell culture supernatants identified by PLS-DA model showing differences between offspring and partners from the LLS.

Metabolite	δ [ppm][a]	Relative difference offspring vs partner[b]	VIP[c]
Energy Metabolism			
Ala-gln	2.34, 1.54	0.95	1.30, 1.37
Alanine	1.50	1.02	2.67
Glucose	5.22, 3.90		1.51, 2.10
	3.78, 3.70	0.99	1.64, 2.65
	3.50, 3.42		1.62, 3.22
Glutamine	2.46	1.02	2.88
Pyroglutamate	4.18, 2.42	1.03	0.55, 0.15
Pyruvate	2.38	0.98	0.83
Lactate	4.10,1.34	1.03	1.52,10.62

[a] mean value of corresponding bucket

[b] as determined from mean spectra of corresponding classes

[c] Importance of contribution values of buckets generated from corresponding PLS-DA model

Discussion

Our main finding is that fibroblast strains derived from offspring of nonagenarian siblings show different levels of metabolites in their cell culture supernatants when compared with those of their partners. The ala-gln and glucose consumption was higher for fibroblast strains derived from offspring when compared with strains of their partners. Also, production of glutamine, alanine, lactate and pyroglutamic acid was found to be higher for fibroblast strains derived from offspring.

Changes in metabolic footprinting of fibroblast strains dependent on the incubation period

Between 24 hours and five days of incubation in serum-free medium, the cell culture supernatants of all fibroblast strains showed decreased levels of glucose, pyruvate and ala-gln. Furthermore, all supernatants showed decreased levels of the essential amino acids

valine, leucine, isoleucine, serine and lysine, consistent with the literature (23). After five days of incubation, levels of glutamine, alanine, lactate and pyroglutamic acid had increased in supernatants of all fibroblast strains.

The ala-gln dipeptide is an important additive in cell culture medium and an important source of glutamine and alanine (24). Increasing levels of glutamine and alanine in the cell culture supernatants could be the result of the intracellular enzymatic digestion of the ala-gln dipeptide (24), after which the excess of both amino acids (i.e. not needed for metabolism) is excreted back into the medium. This would also account for the decrease of ala-gln.
When available, glucose is the main source of energy of cells, explaining the decreasing levels of glucose in the cell culture supernatants of the fibroblast strains. Through the glucose-alanine cycle (25), alanine can be formed from glucose, possibly contributing to the increased levels of alanine observed in the cell culture supernatants. Indeed, it was reported earlier that in addition to the formation of lactic acid, alanine and glutamic acid are secreted into medium by murine fibroblasts (26). Furthermore, human fibroblasts were reported to convert a large proportion of glutamine in culture medium to lactate (27), dependent on cell density (23).

Different metabolic footprint profile of fibroblast strains from longevity family members

The ala-gln and glucose consumption was higher for fibroblast strains derived from offspring of nonagenarian siblings, when compared with fibroblast strains from their partners. Indeed, earlier we showed that serum glucose metabolism and insulin sensitivity is different for the long-living families (4;5). Indeed, earlier we showed that, *in vivo*, the offspring group showed lower levels of thyroid hormone (T3 and T4) (10). Since thyroid hormone stimulates lipid metabolism (28), these data suggest that fibroblast strains from offspring have a lower lipid metabolism. It is also important to realize that the fibroblast strains were cultured in serum-free medium. Serum is an important source of lipids in cell culture medium, so when it is removed, glucose will be the main energy substrate available. Since the fibroblast strains of offspring showed a higher glucose consumption, they might be better able to adapt to the serum free conditions when compared with the strains of the partners.

Production of glutamine, alanine, lactate and pyroglutamic acid was found to be higher for fibroblast strains derived from offspring, when compared with fibroblast strains from partners. The higher production of glutamine and alanine is consistent with the higher consumption of ala-gln and glucose since these are interconverted into each other by glycolysis and the glucose-alanine cycle.

Research into the disease lactiacidemia has implied the role of mitochondrial function in serum lactate levels (29;30). The higher glucose-consumption in strains from offspring is consistent with the finding that respiration-deficient fibroblasts show a higher constitutive rate of glucose transport (31), since we found earlier that strains from offspring are more sensitive to inhibition of the respiratory chain by rotenone, when compared with strains of partners (7;8). Fibroblast strains from offspring were more prone to go into rotenone-induced apoptosis, but showed less rotenone-induced senescence. Also, strains from offspring showed a stronger rotenone-induced decrease in growth rate.

Metabolites in energy metabolism have also been connected to cell damage, cell cycle, apoptosis and senescence. Lactate levels inhibit cell proliferation (32;33) and lactate dehydrogenase (LDH) mediates apoptosis in glucose-starved c-Myc transformed cells (34;35). High glucose levels have been shown to induce senescence in human fibroblasts (36). Fibroblast strains from offspring are more prone to go into stress-induced apoptosis but show less senescence when compared with strains from partners (7). This is consistent with the fact that we found lower levels of glucose for strains from offspring and could be explained by a process called hysteresis, described as metabolite-induced gene expression of the metabolic machinery, creating a molecular memory (11).

In vitro models to study metabolism

In vitro, the kinetics of metabolism are very much dependent on cell culture conditions. It has been suggested that treatments that induce cell proliferation activate enzymatic pathways leading to the formation of lactate (37). Removal of serum, as in our experiments, usually inhibits cell proliferation, implying decreased lactate production. Yet, fibroblast strains from offspring showed higher levels of lactate in the medium than those of their partners, possibly because strains from offspring are less sensitive to removal of factors which promote proliferation. Furthermore, serum starvation-induced quiescent cells are resistant to

becoming senescent (38). As already alluded to, we showed that fibroblasts strains from offspring are indeed less sensitive to (stress-induced) senescence (7).

Manipulation of single genes in model organisms has provided much insight in to the pathways regulating metabolism. Evidently, this genetic manipulation is limited in humans *in vivo* for ethical reasons. It is, however, possible to experiment with cells isolated from humans, providing a powerful tool to study the pathways regulating metabolism. Furthermore, it is difficult to measure metabolites at the cellular level in organisms *in vivo*, whereas this is much easier for cells *in vitro*. Care should be taken, though, in translating *in vitro* results to the *in vivo* situation, for two main reasons. First, *in vitro* characteristics of cells depend on culture conditions like the type of medium, batch and concentration of added serum, oxygen concentration and the number of PDs undergone *in vitro*, making it difficult to compare studies (39). Second, cells *in vitro* have been removed from their natural environment, being derived from many factors in the blood (e.g. cytokines and growth factors) and cell-cell and cell-matrix interactions (40). Despite these caveats, *in vitro* cultured cells derived from subjects of different populations reflect differences between these subjects, providing a powerful tool to study differences in metabolism between these subjects at the cellular level

An important strength of our study is the large number of fibroblast strains obtained from subjects of various biological ages, collected and stored in a highly standardized manner. An important limitation of this study is the fact that the observed differences were small and that, despite being valid, the predictive power of the model proved limited. This may be due to the fact that not all offspring carry the longevity traits and hence the observation in the fibroblasts of a random group of offspring dilutes the effects of longevity associated mechanisms that could be observed. In addition, compounds present at much lower concentrations could be responsible for metabolic differences between fibroblast strains from offspring and partners, but the methods applied here were not sensitive enough to detect differences in these compounds.

In conclusion, we report for the first time, that the NMR-based metabolic profiles of human cells *in vitro* reflect the propensity for human longevity of the subjects from whom these were

derived. Future work will have to elucidate the enzymes driving differences in metabolism and the pathways regulating these enzymes.

Reference List

(1) Oeppen J, Vaupel JW. Demography. Broken limits to life expectancy. Science 2002;296:1029-1031.

(2) Schoenmaker M, de Craen AJ, de Meijer PH, Beekman M, Blauw GJ, Slagboom PE, Westendorp RG. Evidence of genetic enrichment for exceptional survival using a family approach: the Leiden Longevity Study. Eur J Hum Genet 2006;14:79-84.

(3) Westendorp RG, van Heemst D, Rozing MP, Frolich M, Mooijaart SP, Blauw GJ, Beekman M, Heijmans BT, de Craen AJ, Slagboom PE. Nonagenarian siblings and their offspring display lower risk of mortality and morbidity than sporadic nonagenarians: The Leiden Longevity Study. J Am Ger Soc 2009;57:1634-1637.

(4) Rozing MP, Westendorp RG, de Craen AJ, Frolich M, de Goeij MC, Heijmans BT, Beekman M, Wijsman CA, Mooijaart SP, Blauw GJ, Slagboom PE, van HD. Favorable glucose tolerance and lower prevalence of metabolic syndrome in offspring without diabetes mellitus of nonagenarian siblings: the Leiden longevity study. J Am Geriatr Soc 2010;58:564-569.

(5) Wijsman CA, Rozing MP, Streefland TC, Le CS, Mooijaart SP, Slagboom PE, Westendorp RG, Pijl H, van HD. Familial longevity is marked by enhanced insulin sensitivity. Aging Cell 2010;10-9726.

(6) Vaarhorst AA, Beekman M, Suchiman EH, van HD, Houwing-Duistermaat JJ, Westendorp RG, Slagboom PE, Heijmans BT. Lipid metabolism in long-lived families: the Leiden Longevity Study. Age (Dordr) 2010.

(7) Dekker P, Maier AB, van HD, de Koning-Treurniet C, Blom J, Dirks RW, Tanke HJ, Westendorp RG. Stress-induced responses of human skin fibroblasts in vitro reflect human longevity. Aging Cell 2009;8:595-603.

(8) Dekker P, van Baalen LM, Dirks RW, Slagboom PE, van Heemst D, Tanke HJ, Westendorp RGJ, Maier AB. Chronic inhibition of the respiratory chain differentially affects fibroblast strains from young and old subjects. J Gerontol A Biol Sci Med Sci 2011 Nov 10 [Epub ahead of print].

(9) Derhovanessian E, Maier AB, Beck R, Jahn G, Hahnel K, Slagboom PE, de Craen AJ, Westendorp RG, Pawelec G. Hallmark features of immunosenescence are absent in familial longevity. J Immunol 2010;185:4618-4624.

(10) Rozing MP, Westendorp RG, de Craen AJ, Frolich M, Heijmans BT, Beekman M, Wijsman C, Mooijaart SP, Blauw GJ, Slagboom PE, van HD. Low serum free triiodothyronine levels mark familial longevity: the Leiden Longevity Study. J Gerontol A Biol Sci Med Sci 2010;65:365-368.

(11) Mobbs CV, Mastaitis JW, Zhang M, Isoda F, Cheng H, Yen K. Secrets of the lac operon. Glucose hysteresis as a mechanism in dietary restriction, aging and disease. Interdiscip Top Gerontol 2007;35:39-68.:39-68.

(12) Kell DB, Brown M, Davey HM, Dunn WB, Spasic I, Oliver SG. Metabolic footprinting and systems biology: the medium is the message. Nat Rev Microbiol 2005;3:557-565.

(13) MacIntyre DA, Melguizo SD, Jimenez B, Moreno R, Stojkovic M, Pineda-Lucena A. Characterisation of human embryonic stem cells conditioning media by 1H-nuclear magnetic resonance spectroscopy. PLoS One 2011;6:e16732.

(14) Bradley SA, Ouyang A, Purdie J, Smitka TA, Wang T, Kaerner A. Fermentanomics: monitoring mammalian cell cultures with NMR spectroscopy. J Am Chem Soc 2010;132:9531-9533.

(15) Maier AB, le Cessie S, Koning-Treurniet C, Blom J, Westendorp RG, van Heemst D. Persistence of high-replicative capacity in cultured fibroblasts from nonagenarians. Aging Cell 2007;6:27-33.

(16) Keun HC, Ebbels TM, Antti H, Bollard ME, Beckonert O, Schlotterbeck G, Senn H, Niederhauser U, Holmes E, Lindon JC, Nicholson JK. Analytical reproducibility in (1)H NMR-based metabonomic urinalysis. Chem Res Toxicol 2002;15:1380-1386.

(17) Kumar A, Ernst RR, Wuthrich K. A two-dimensional nuclear Overhauser enhancement (2D NOE) experiment for the elucidation of complete proton-proton cross-relaxation networks in biological macromolecules. Biochem Biophys Res Commun 1980;95:1-6.

(18) Price WS. Water signal suppression in NMR spectroscopy. 1999: 289-354. Ref Type: Book, Whole.

(19) Wu PS, Otting G. Rapid pulse length determination in high-resolution NMR. J Magn Reson 2005;176:115-119.

(20) Coron A, Vanhamme L, Antoine JP, Van HP, Van HS. The filtering approach to solvent peak suppression in MRS: a critical review. J Magn Reson 2001;152:26-40.

(21) Torgrip RJO, Aberg KM, Alm E, Schuppe-Koistinen I, Lindberg J. A note on normalization of biofluid 1D H-1-NMR data. Metabolomics 2008;4:114-121.

(22) Dieterle F, Ross A, Schlotterbeck G, Senn H. Probabilistic quotient normalization as robust method to account for dilution of complex biological mixtures. Application in 1H NMR metabonomics. Anal Chem 2006;78:4281-4290.

(23) Lemonnier F, Gautier M, Moatti N, Lemonnier A. Comparative study of extracellular amino acids in culture of human liver and fibroblastic cells. In Vitro 1976;12:460-466.

(24) Yagasaki M, Hashimoto S. Synthesis and application of dipeptides; current status and perspectives. Appl Microbiol Biotechnol 2008;81:13-22.

(25) Felig P. The glucose-alanine cycle. Metabolism 1973;22:179-207.

(26) Lanks KW. End products of glucose and glutamine metabolism by L929 cells. J Biol Chem 1987;262:10093-10097.

(27) Zielke HR, Sumbilla CM, Sevdalian DA, Hawkins RL, Ozand PT. Lactate: a major product of glutamine metabolism by human diploid fibroblasts. J Cell Physiol 1980;104:433-441.

(28) Pucci E, Chiovato L, Pinchera A. Thyroid and lipid metabolism. Int J Obes Relat Metab Disord 2000;24 Suppl 2:S109-12.:S109-S112.

(29) Robinson BH. Cell culture studies on patients with mitochondrial diseases: molecular defects in pyruvate dehydrogenase. J Bioenerg Biomembr 1988;20:313-323.

(30) Robinson BH, McKay N, Goodyer P, Lancaster G. Defective intramitochondrial NADH oxidation in skin fibroblasts from an infant with fatal neonatal lacticacidemia. Am J Hum Genet 1985;37:938-946.

(31) Andrejchyshyn S, Continelli L, Germinario RJ. Permanent hexose transport upregulation in a respiration-deficient human fibroblast cell strain. Am J Physiol 1991;261:C973-C979.

(32) Hehenberger K, Heilborn JD, Brismar K, Hansson A. Inhibited proliferation of fibroblasts derived from chronic diabetic wounds and normal dermal fibroblasts treated with high glucose is associated with increased formation of l-lactate. Wound Repair Regen 1998;6:135-141.

(33) Yevdokimova NY, Podpryatov SE. Hyaluronic acid production and CD44 expression in cultured dermal fibroblasts of patients with non-insulin-dependent diabetes mellitus with and without chronic ulcers on the lower extremity. Wound Repair Regen 2005;13:181-188.

(34) Shim H, Chun YS, Lewis BC, Dang CV. A unique glucose-dependent apoptotic pathway induced by c-Myc. P Natl Acad Sci USA 1998;95:1511-1516.

(35) Dorai H, Kyung YS, Ellis D, Kinney C, Lin C, Jan D, Moore G, Betenbaugh MJ. Expression of anti-apoptosis genes alters lactate metabolism of Chinese Hamster Ovary cells in culture. Biotechnol Bioeng 2009;103:592-608.

(36) Blazer S, Khankin E, Segev Y, Ofir R, Yalon-Hacohen M, Kra-Oz Z, Gottfried Y, Larisch S, Skorecki KL. High glucose-induced replicative senescence: point of no return and effect of telomerase. Biochem Biophys Res Commun 2002;296:93-101.

(37) Fodge DW, Rubin H. Stimulation of lactic acid production in chick embryo fibroblasts by serum and high pH in the absence of external glucose. J Cell Physiol 1975;86:453-457.

(38) Demidenko ZN, Blagosklonny MV. Growth stimulation leads to cellular senescence when the cell cycle is blocked. Cell Cycle 2008;7:3355-3361.

(39) Macieira-Coelho A. Relevance of in vitro studies for aging of the organism. A review. Z Gerontol Geriatr 2001;34:429-436.

(40) Horrobin DF. Modern biomedical research: an internally self-consistent universe with little contact with medical reality? Nat Rev Drug Discov 2003;2:151-154.

Supplemental material

Supplemental table 1. Outlier identification: Characteristics of Spectroscopic Outliers

#	Sample ID	TSP line width	Water Suppression
89	Sample missing	-	-
91	Sample missing	-	-
109	50-24h	Acquisition failed	-
169	111-24h	OK (1.03 Hz)	FAIL
195	117-5d	FAIL (4.06 Hz)	OK
197	118-24h	FAIL (6.56 Hz)	OK
199	118-5d	FAIL (3.44 Hz)	OK
203	119-5d	FAIL (3.19 Hz)	OK
207	120-5d	OK (1.15 Hz)	FAIL
235	127-5d	OK (0.82 Hz)	FAIL
287	121-128-control-5d	FAIL (7.43 Hz)	OK
289	129-136-control-24h	FAIL (1.56 Hz)	FAIL

Visual inspection of the individual spectra during data processing was used to remove spectroscopic outliers. As parameter for shim quality, the half width of the TSP line was evaluated after processing without apodization. Water suppression quality was assessed by total height of the remaining water resonance and presence of shoulders at the base of the signal. A total of 10 datasets were removed prior to further analysis as summarized in Supplemental table1. Biological outliers were identified based on Hotelling's T2 range (above 99% T2 critical value) and distance of the observation in the training set to the X model plane values (> 2) (These parameters describe how well the data is located within model space).

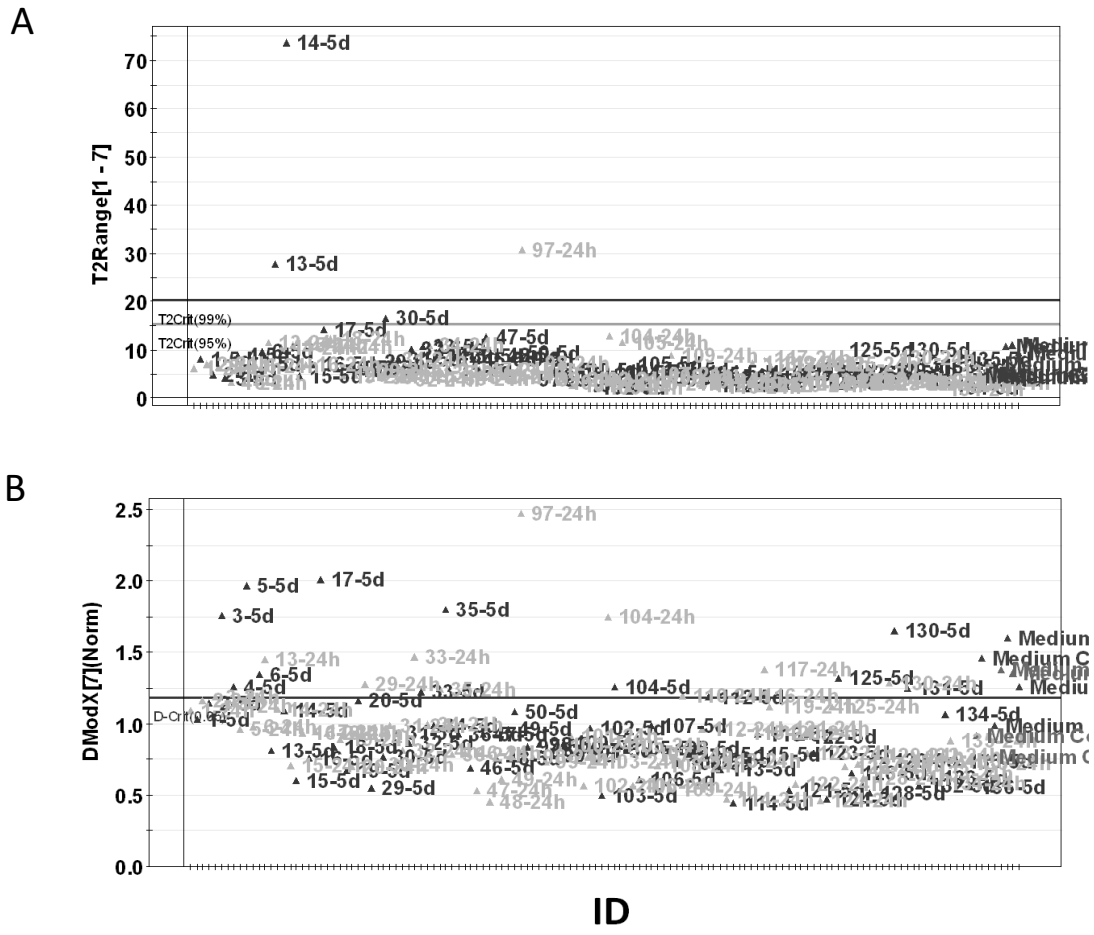

Supplemental figure 1. Hotelling's T2 plot (A) and DModX plot (B) for PCA model built using eight components from data without scaling of variables. Data points are labeled according to fibroblast culture incubation duration of 24 hours (▲) and five days (▲) as well as control medium incubated for 24 hours (▲) and five days (▲).

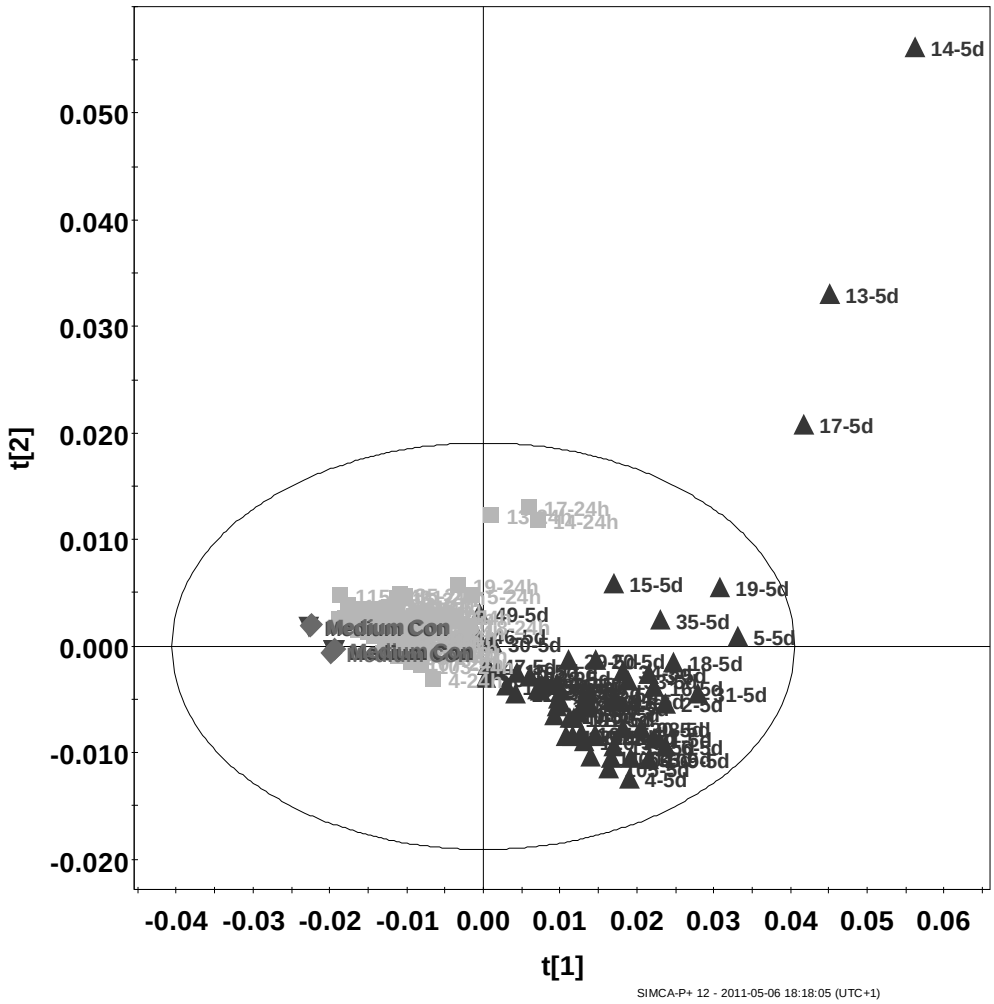

Supplemental figure 2. Scores plot of first two principal components from PCA model built from complete data set without scaling of variables. Data points are labeled according to fibroblast culture incubation duration of 24 hours (■) and five days (▲) as well as cell-free/serum-free medium (control medium) incubated for 24 hours (◆) and five days (▼).

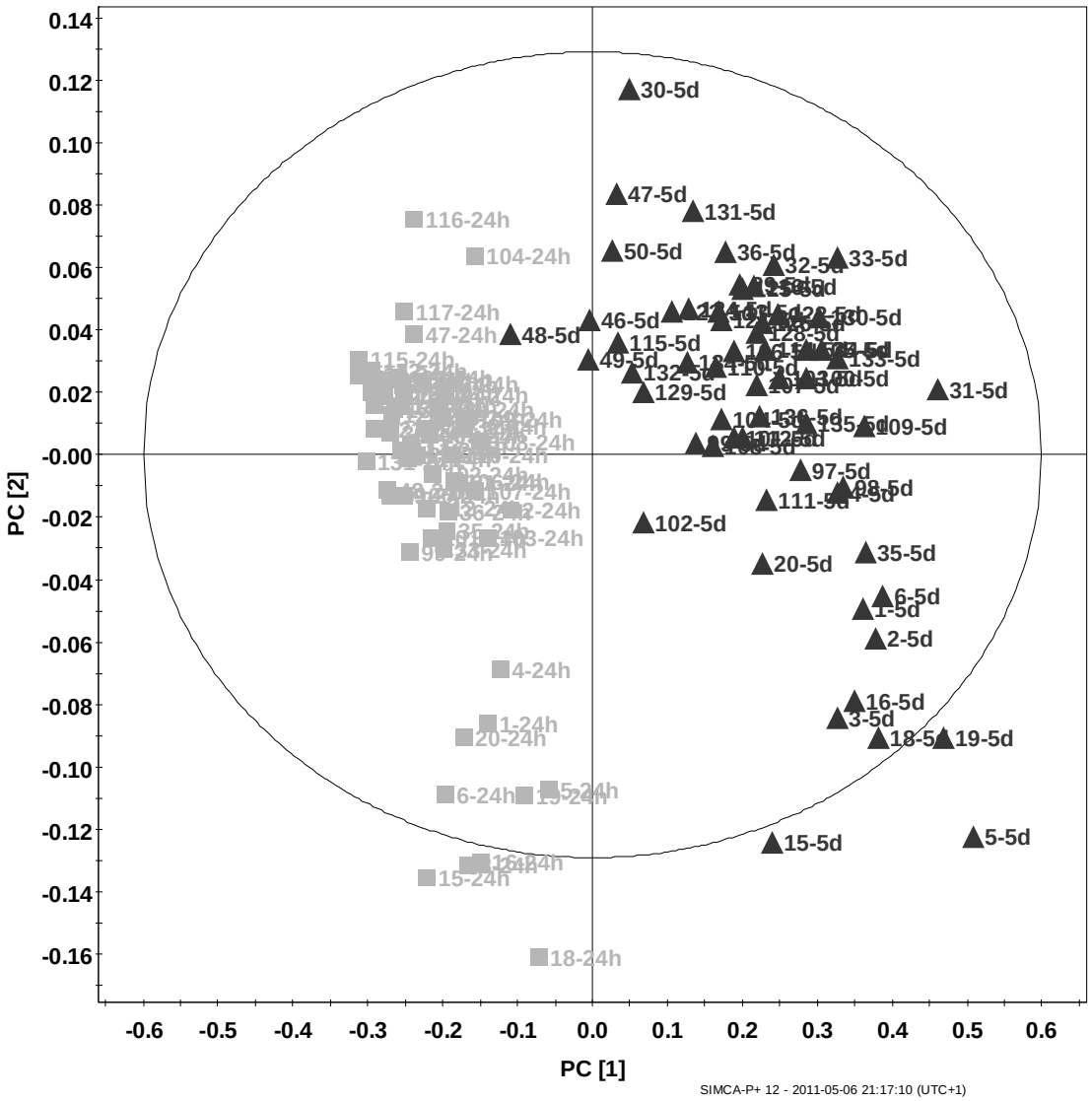

Supplemental figure 3. Scores plot of first two components from PLS-DA model built using time point as response variable. Data points are labeled according to fibroblast culture incubation duration of 24 hours (■) and five days (▲), respectively.

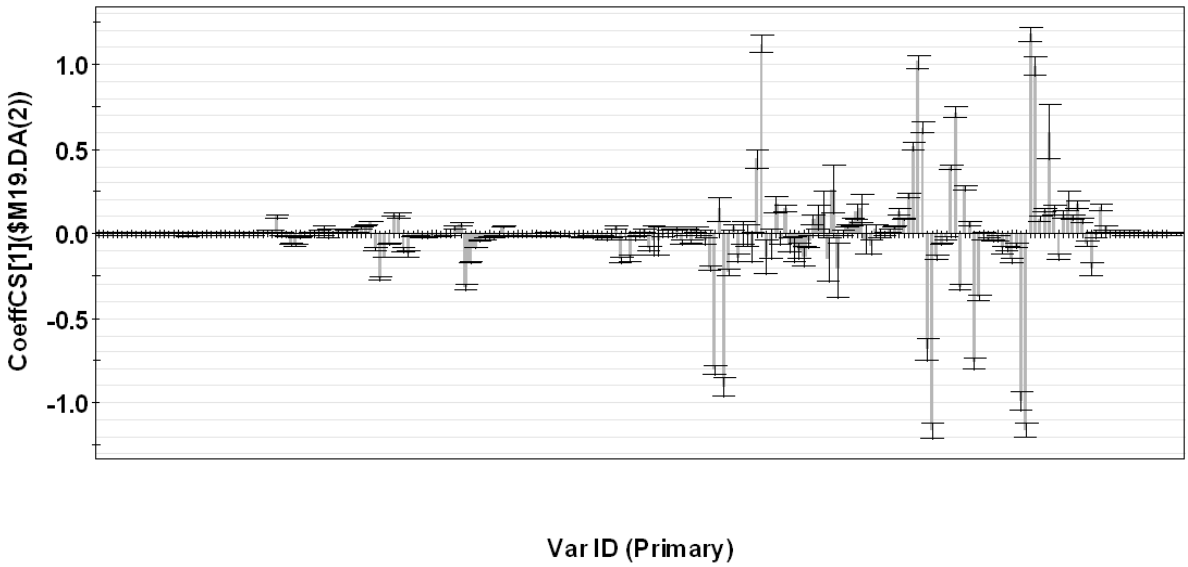

Supplemental figure 4. Coefficients plot for first component of PLS-DA model built using time point as response variable.

OSC Validation

For validation of the OSC filtering step, 59 datasets were generated using OSC filtering of the original data leaving out one of the 59 observations, such that each sample was omitted once (leave-one-out cross validation). For each dataset an independent PLS-DA two-class models was build using the 58 observations that were included in the filtering step followed by prediction of the response variable for the excluded observation using the respective model. The predicted values were then used for classification of the samples as summarized in Supplemental table 2. The overall correct classification of all samples was 62.7% with a 95% confidence interval for the proportion correctly identified of [0.5036, 0.7504] excluding the null hypothesis.

Supplemental table 2. Misclassification table for OSC leave-one-out cross validation

			predicted	
	Members	Correct	offspring	partner
offspring	28	60.7%	17	11
partner	31	64.5%	11	20
Total	**59**	**62.7%**	**28**	**31**

.